Accurate calculations of reaction rates: Predictive theory based on a rigorous quantum transition state concept

Uwe Manthe

Accurate calculations of reaction rates:
Predictive theory based on a rigorous quantum transition state concept

SCHOLARONE™
Manuscripts

Topical Review

Accurate calculations of reaction rates: Predictive theory based on a rigorous quantum transition state concept

Uwe Manthe

Theoretische Chemie, Fakultät für Chemie, Universität Bielefeld,
Universitätsstr. 25, D-33615 Bielefeld, Germany

(*Received 00 Month 200x; final version received 00 Month 200x*)

In recent years the accurate and truly predictive calculation of thermal rate constants has become feasible for reactive systems consisting of more than only three or four atoms and results for benchmark six atom reactions as $H+CH_4 \rightarrow H_2+CH_3$ were presented. The present article reviews research focusing on the accurate calculation of rates for reactions proceeding via barriers and highlights key method developments as well as important applications in the area. It discusses the quantum transition state concept which allows one to rigorously and efficiently compute averages with respect to thermal or micro-canonical ensembles and to interpret the results using intuitive pictures. Schemes for the construction of accurate high-dimensional potential energy surfaces required in quantum dynamics simulations and for performing efficient multi-dimensional wave packet dynamics calculations are also reviewed. As a results of the large number of accurate reaction rate calculations for diverse reactions which has been presented in about the last decade, a consistent picture of the importance of quantum effects in reaction rates emerged. The present article attempts to comprehensively describe this picture and in addition will try to provide guidelines when significant deviations for classical (harmonic) transition state theory can be excepted.

1.   Introduction

The last two decades have seen significant progress in the accurate simulation and detailed understanding of elementary chemical reaction processes. Considering the most fundamental and precise level of theory, the accurate description even of seemingly simple chemical reactions is a challenging task: quantum effects as tunneling or zero point energy have to be incorporated in the description of the motion of the atoms during the reaction process, particularly if reactions including the transfer of hydrogen atoms or protons are considered. Then the delocalized nature of quantum mechanics, most prominently reflected in the Heisenberg uncertainty principle, requires the knowledge of extended regions of the underlying electronic potential energy surface (PES) of the molecular system. Furthermore the complex nature of the chemical reaction process typically results in strong couplings between several degrees of freedom and requires multi-dimensional PESs and quantum dynamics simulations. Consequently, the use of dimensionality reducing approximations is highly problematic and full-dimensional quantum mechanical calculations are required if one aims at reliable theoretical predictions.

The first rigorous, i.e. full-dimensional quantum mechanical, calculations studying a chemical reaction was published in 1976 [1]. Here the simple-most chemical reaction, the $H + H_2 \rightarrow H_2 + H$ hydrogen exchange, was investigated. Further progress from triatomic reactions towards polyatomic reactions faced a central

E-mail: uwe.manthe@uni-bielefeld.de

problem: the exponential scaling of the numerical effort of grid or basis set based numerical techniques with the dimensionality. The first full six-dimensional quantum calculation for four atom reactions only appeared in the early 1990's [2–4] studying the $H_2 + OH \rightarrow H + H_2O$ reaction. The step beyond tetratomic reaction was then taken already in 2000 [5] when full-dimensional quantum dynamics calculations for a six atom reaction, $H + CH_4 \rightarrow H_2 + CH_3$, were presented for the first time. It should be noted that the first such calculations for a tetratomic reaction [2] as well as for a six atom reaction [5] explicitly focused on the calculation of reaction rates. Thus, rigorous reaction rate calculations have a pioneering role in the quest towards the accurate description of increasing complex reactions. Besides the focus on selected observables as reaction rates [2, 5] or initial state-selected reaction probabilities [3, 4, 6, 7] (the first full-dimensional quantum dynamics calculation of initial state-selected reaction probabilities for a six atom reaction appeared just recently [6, 7]), the development of efficient schemes for the multi-dimensional wave packet propagation, particularly the multi-configurational time-dependent Hartree (MCTDH) approach [8, 9], contributed significantly to the progress.

Thermal rate constants are generally the magnitudes most relevant for a chemist investigating a reaction. A theoretical approach focusing on the accurate calculation of rate constants is thus well adapted towards the needs of research in chemistry. Considering chemistry in general, *transition state theory* (TST) provides the central framework dominating a chemists thinking about reaction rates. It is therefore particularly interesting to note that the above mentioned rigorous reaction rate calculations [2, 5] employ concepts [10–12] which can be viewed as a rigorously correct, quantum mechanical generalization of the transition state (TS) approach. Thus, these reaction rate calculations do not only provide accurate reaction rate data but can also help to understand quantum effects in reaction dynamics using intuitive pictures derived from a *quantum transition state concept*.

The present article reviews research focusing on the accurate calculations of reaction rates employing rigorous theory. It does not attempt to cover approximate approaches based on (quantum) transition state ideas. There is a variety of such approaches and detailed comparisons of their results with rigorous reaction rate calculations reviewed here have been published [13–16]. Furthermore, we will restrict our attention to reaction proceeding via potential barrier or through a similar dynamical bottleneck. In these situation the passage of the reaction barrier is the central step of the reaction process and a transition state picture provides physically adequate description. Elementary reactions proceeding not via barriers but via potential wells causing long-living intermediates show very different dynamical behavior. Here transition state based concepts are physically inadequate. The efficient treatment of such reaction requires different concepts, e.g. combined statistical and capture approaches [17], which will not be reviewed here.

Accurate reaction rate calculations can be divided in three tasks which have to be addressed: first electronic structure calculations must accurately compute electronic energies at given geometries, then a multi-dimensional PES has to be constructed based on the electronic structure data, and finally thermal rate constants must be obtained from accurate quantum dynamics simulations on this PES. The methodology of ab initio electronic structure calculations is a highly developed area of research with distinct character, therefore the present review will not address this part required in reaction rate calculations explicitly. It only should be noted that highly accurate electronic structure calculations are required to predict thermal rate constants of chemical reactions: due to the $e^{-E/k_B T}$ Boltzmann factor present in the theory of thermal rates, energy differences are always measured relative to the thermal energy $k_B T$. Relevant predictions thus require to computed electronic

energies significantly more accurate than k_BT which at room temperature takes values of $k_BT \approx 1\ mHartree \approx 0.025\ eV \approx 0.6\ kcal/mol \approx 2\ kJ/mol \approx 200\ cm^{-1}$. While this clearly is a demanding task, these accuracies have been achieved in recent reaction rate calculations studying the $H + CH_4 \rightarrow H_2 + CH_3$ reaction [18, 19].

Theoretical concepts, results, and important implications of rigorous reaction rate calculations are reviewed in Sect.2. First, the central steps in the development of the quantum transition state concept are described. Then the advance in applications from triatomic systems to six atom reactions as well as reactions on surfaces and in condensed phase is reviewed. Relevant techniques which contributed to this progress will be briefly explained subsequently. Finally central conclusions relevant for a wider chemical community are discussed: When can quantum effects expected to be important? What is the impact of zero point energy and tunneling? Is the separation of internal motion and overall rotation a good approximation?

The construction of multi-dimensional PESs required in accurate reaction rate calculations is another central topic which is reviewed in Sect.3. The methods and ideas which formed the basis for the tremendous progress in this area in the last decade are first described in a general context. Then specific aspects of the construction of PESs for reaction rate calculations are discussed. It is highlighted that efficient schemes for the PES constructions in the reaction rate context are "semidirect" in character, relate to the quantum transition state concept, and require only a moderate number of ab initio data points even for polyatomic reactions showing many degrees of freedom.

The article closes with a final section discussing conclusions and future perspectives of reaction rate calculations and the investigation of mode-specific reaction dynamics based on the quantum transition state concept.

2. Reaction rates: quantum dynamics

2.1. *Rigorous quantum transition state concept*

Quantum scattering calculations computing the scattering matrix yield a fully state-specific description of chemical reaction processes. Wave packet dynamics calculations which simulate the dynamics of a wave packet moving from the reactant asymptotic region towards the product asymptotic region can provide a similar wealth of information about the reaction process. Aiming at the calculation and understanding of the thermal rate constant $k(T)$ of a chemical reaction, a different strategy is more rewarding: $k(T)$ is determined by the passage of the reaction barrier and a state-specific description referencing explicitly to quantum states of the reactant or product is not required to compute or physically interpret $k(T)$. Concepts taken from statistical mechanics and dynamical simulations restricted to the barrier region provide a more intuitive and numerically more efficient description. Classical transition state theory (TST) is based on these ideas and the importance of TST for a general chemists understanding of elementary reaction processes can hardly be overestimated. However, TST is an approximate theory and the present review focuses on the rigorous calculation of reaction rates.

Flux correlation functions, introduced in their quantum mechanical formulations by Yamamoto [20] and Miller and coworkers [10, 11], provide the rigorous theoretical framework to compute reaction rates based on statistical mechanical concepts without reference to asymptotic reactant or product states. There is a variety of specific flux correlation functions using energy as well as time-dependent representations. The connection to TST can nicely be seen employing a flux position

4

correlation function [10]:

$$k(T) = \frac{1}{Q_r(T)} \lim_{t \to \infty} tr \left(e^{-\frac{\hat{H}}{k_B T}} \hat{F} \; e^{i\hat{H}t} \; h \; e^{-i\hat{H}t} \right) \tag{1}$$

(Please note that $\hbar = 1$ is used throughout this article.) Here $\hat{H}$ is the Hamiltonian, $Q_r(T)$ is the partition function of the reactants, and h specifies the dividing surface which separates reactant and product geometries. h equals unity on the product side of the dividing surface, and vanishes on the reactant side. The flux operator $\hat{F} = i[\hat{H}, h]$ measures the flux through the dividing surface. Eq.(1) implies a transition state based interpretation of the reaction process: considering the full thermal ensemble, $\frac{1}{Q_r(T)} tr \left(e^{-\frac{\hat{H}}{k_B T}} ... \right)$, the thermal rate constant is given by the flux through the dividing surface, which will finally end up as product in the infinite future (for a more detailed explanation of the theory and its connections to TST see, e.g., previous reviews [21–25]). The numerically most efficient approaches typically do not compute the thermal rates directly but employ the cumulative reaction probability $N(E)$ which is related to $k(T)$ via Boltzmann averaging:

$$k(T) = \frac{1}{2\pi \; Q_r(T)} \int dE \; N(E) \; e^{-\frac{E}{k_B T}} \; . \tag{2}$$

Flux correlation functions for the calculation of $N(E)$ can be derived based on the flux correlation formula of Miller et al. [11],

$$N(E) = 2\pi^2 \; tr \left(\hat{F} \; \delta(\hat{H} - E) \; \hat{F} \; \delta(\hat{H} - E) \right) \; . \tag{3}$$

As seen in Eqs.(1) and (3), the calculation of $k(T)$ or $N(E)$ via flux correlation functions requires to compute averages over thermal or micro-canonical ensembles. These averages are represented by the traces present in the above expressions. Their evaluation presented a major computational problem which initial work utilizing flux correlation functions faced. The straightforward evaluation of the trace employing a complete basis set ψ_j, $tr(\hat{A}) = \sum_{j=1}^{N} < \psi_j | \hat{A} | \psi_j >$, is infeasible even for medium sized problems due to the large size N of the basis set required. Using the specific properties of the flux operator [26] to avoid tracing over the reaction coordinate can not really solve this problem: considering a f-dimensional problem tracing with respect in the other (f-1) coordinates still has to be done. Consequently, early quantum calculations using flux correlation functions [26–38] were restricted to systems not exceeding three atoms.

While flux correlation functions immediately relate the reaction rate to the quantum dynamics in the vicinity of the reaction barrier and thus provide a first connection to transition state idea, another concept taken from transition state theory can be used to address the problem posted by the thermal or micro-canonical ensemble averages required. This has first been demonstrated in Ref.[12]: rewriting Eq.(3) as $N(E) = tr(\hat{P}(E))$ a hermitian, positive semidefinite operator $\hat{P}(E)$ called *reaction probability operator* had been introduced. Investigating the $H + H_2$ reaction for vanishing total angular momentum $J = 0$, $\hat{P}(E)$ was found to have only a very small number of non-vanishing eigenvalues which can straightforwardly be interpreted as the contributions of the different vibrational states of the activated complex. Since the number of relevant vibrational states of the activated complex contributing to the reaction rate at relevant temperatures or energies is typically small, only few quantum states contribute relevantly to the thermal or micro-canonical ensemble

averages in the flux correlation functions (for $J = 0$). Thus, the operator within the trace is of low rank and its eigenvalues can efficiently be computed by iterative diagonalization employing a Lanczos scheme.

Building on this conceptional basis and sparked by the successful application of these ideas to the four atom reaction $H_2 + OH \rightarrow H + H_2O$ [2, 39], a variety of approaches for the rigorous and efficient calculation of reaction rates had been developed subsequently [40–52]. Important steps taken in the development towards the presently employed approaches should be noted: First, the theory has been reformulated in time domain and wave packet propagation techniques have been employed [40, 41]. Second, the schemes for the construction of the wave packets describing the vibrational states of the activated complex could be separated from the real time propagation of the wave packets required to compute $N(E)$ and $k(T)$ [43–45]. The developments established two similar schemes as the present state of the art: the thermal flux eigenstate based approach of Refs.[48, 49] (which uses either MCTDH wave packet propagation [48, 53] or standard wave packet propagation schemes [49]) and the transition state wave packet approach of Refs.[43] (used with standard wave packet propagation schemes).

Finally one aspect has been ignored up to now must be added. The above discussion focused on internal motion and mainly considered calculations for vanishing total angular momentum ($J = 0$). Then the number of relevant vibrational states of the activated complex tends to be small for relevant temperatures since the vibrational frequencies are usually much larger than the thermal energy. This situation changes dramatically if rotational motion is considered. Rotational spacings are typically much smaller than thermal energies. Thus, if rotation is included explicitly in the calculation, a large number of rovibrational states has to be considered. Propagating a wave packet for each of these states can post a significant challenge. However, this problem was overcome by utilizing a rigorously correct statistical approach [54, 55] which can correctly account for rotationally excited states without strongly increasing the number of wave packets to be propagated compared to the $J = 0$ case.

2.2.   *From triatomics to polyatomic reactions*

Prior to the step in method development taken in the early 1990s [12], early reaction rate calculations studied selected triatomic reactions. The full-dimensional calculations for the $H_2 + OH \rightarrow H + H_2O$ reaction [2, 39] then presented the first benchmark application utilizing the rigorous quantum transition state concept to its full extend. Here the cumulative reaction probability $N(E)$ has been obtained in converged full-dimensional quantum mechanical calculations. The calculations were restricted to total angular momentum $J = 0$ and the thermal rate constant was obtained in the J-shifting approximation [56] which implies separability of internal motion and overall rotation in the barrier region. Comparison with experiment showed deficiencies in the Schatz-Elgersma PES [57, 58] employed.

After this initial success, the following work extended and further developed the methodology. In these studies, first different triatomic reactions as $H_2 + Cl \rightarrow H + HCl$ [59–61] and $O(^3P) + HCl \rightarrow OH + Cl$ [45, 47, 54, 55, 62] were investigated. Here also contributions for total angular momentum $J > 0$ were considered and the coupling of internal motion and overall rotation were studied. Later reaction rate calculations for the four atom reactions $H_2 + OH \rightarrow H + H_2O$ [48, 63–65], $H_2 + CN \rightarrow H + HCN$ [49, 66], and $HCl + OH \rightarrow Cl + H_2O$ [67] followed. Some of these studies [48, 54, 55, 60, 61, 65, 67] employed the MCTDH approach [8, 9] to efficiently perform the real and imaginary time wave packet propagations required
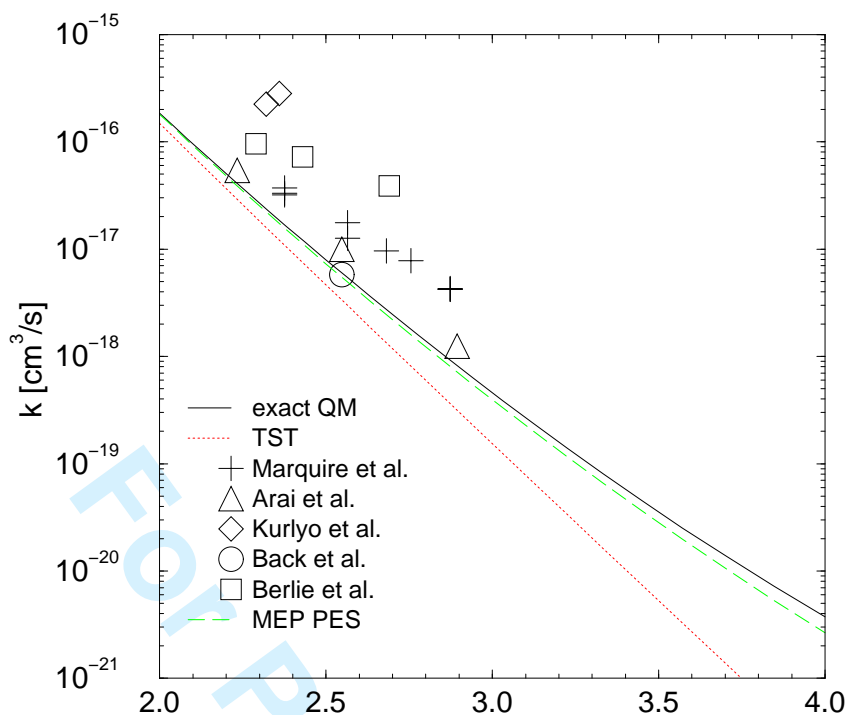
6

Figure 1. Thermal rate constant $k(T)$ of the $H + CH_4 \rightarrow H_2 + CH_3$ reaction [18, 19]: accurate quantum mechanical results and transition state theory results calculated on an accurate ab initio PES are displayed together with experimental results. Results obtained for a the PES which is based only on ab initio data from geometries located at the minimum energy path (MEP) are also shown.

in these calculations.

Based to the combination of MCTDH wave packet propagation and reaction rate calculations via flux correlation functions, larger reactive systems could be investigated in the early 2000s: the first converged full-dimensional quantum dynamics calculation for a six atom reaction studied $N(E)$ and $k(T)$ for $H+CH_4 \rightarrow H_2+CH_3$ [5, 68–70]. Slightly later the reaction $O + CH_4 \rightarrow OH + CH_3$ [71] was investigated on the same level of theory. It should be noted that previous studies of triatomic and tetratomic reaction yielded a detailed understanding of the effects of the overall rotation on thermal rate constants, so that these calculations could safely be restricted to total vanishing angular momentum and employed the J-shifting scheme [56].

While the above calculations could treat the quantum dynamics of the reaction process rigorously, still the underlying PES used in these calculations [72, 73] were not accurate and resulted in significant differences between experiment and theory. Therefore the further development considered the construction of accurate full-dimensional PES which will be discussed in some more detail in Sect.3. A new accurate PES was constructed for the $H + CH_4 \rightarrow H_2 + CH_3$ reaction and truly accurate reaction rates were obtained performing rigorous full-dimensional quantum dynamics calculation on this PES [18, 19]. Considering careful error estimates for all steps of the theoretical description, one could conclude that the accuracy of the computed rates was at least comparable to the accuracy of the experimental data available (see Fig.1 for an Arrhenius plot of the computed and experimental rate constants). Later on, also $k(T)$'s and $N(E)$'s for isotopic analog reaction $D + CH_4 \rightarrow HD + CH_3$ [74] and the reverse reactions $H_2 + CH_3 \rightarrow H + CH_4$ and $D_2 + CH_3 \rightarrow D + CH_3D$ [75] were calculated on the same level of theory.

Beside the investigation of gas phase systems (here further calculations ranging from triatomic [76, 77] to hexatomic reactions [78–80] could be mentioned) also rates for process on surfaces [81, 82] and reactions in condensed phase [83, 84] were

studied based on the quantum transition state concept. The dissociative adsorption of N_2 on a stepped Ru-surface was studied by 6D quantum dynamics calculations for a rigid Ru-surface [82] and the effect of surface motion on in the system was considered on TST level [85]. The rates for hydrogen diffusion on a Cu surface where computed quantum mechanically including the treatment of Cu surface vibration [81]. A standard model for solid state physics, a double well system coupled bilinear to a bath, was rigorously treated using the quantum transition state concept and (multi-layer) MCTDH calculations [83, 84] by Wang, Thoss, and coworkers. This study extended previous work of Topaler and Makri [86] which relied on real time path integral calculations and offer a perspective to describe the real time quantum dynamics of condensed phase reactions beyond the limitation to harmonic bath models.

2.3.   *Efficient numerical techniques*

In reaction rate calculations based on the quantum transition state concept, wave packets representing the vibrational states of the activated complex are started at the reaction barrier. They are then propagated towards the reactant and product channels. However, the propagation can be stopped as soon as all components of the wave packets have decided whether they will end up either as products or as reactants. For reactions showing significant potential barriers, this point of no return is typically reached after only a few ten femtoseconds. Thus, only short propagation times are required.

The multi-configurational time-dependent Hartree (MCTDH) approach [8, 9] is ideally suited to facilitate numerically exact wave packet propagations under these circumstances. It then allows one to rigorously describe the quantum dynamics of polyatomic systems consisting of more than four or five atoms. The MCTDH approach employs a layered representation or the wavefunction

$$\psi(x_1, .., x_f, t) = \sum_{j_1=1}^{n_1} .. \sum_{j_f=1}^{n_f} A_{j_1..j_f}(t) \prod_{\kappa=1}^{f} \phi_{j_\kappa}^{(\kappa)}(x_\kappa, t) \ ,$$

$$\phi_j^{(\kappa)}(x_\kappa, t) = \sum_{l=1}^{N_\kappa} c_{jl}^{(\kappa)}(t) \cdot \chi_l(x_\kappa) \ . \tag{4}$$

The wavefunction is first represented in a basis of time-dependent expansion functions $\phi_{j_\kappa}^{(\kappa)}(x_\kappa, t)$ which are called single-particle functions. In a second layer of the representation, the single-particle functions are then represented in the basis of the underlying "primitive" time-independent basis functions $\chi_l(x_\kappa)$. Standard discrete variable representation (DVR) [87–89] or fast Fourier transform (FFT) [90] schemes can be used to provide the $\chi_l(x_\kappa)$. The equations of motion which describe the expansion coefficients $A_{j_1..j_f}(t)$ and $c_{jl}^{(\kappa)}(t)$ of both layers can be obtained from the Dirac-Frenkel variational principle. It should be noted that extensions which can further increase the efficiency of the original MCTDH approach utilize the combination of several physical coordinates in a single "logical" coordinate (mode combination MCTDH [91, 92]) and employ more than two layers in the wavefunction representation (multi-layer MCTDH [93–95]).

One further aspect of the MCTDH approach is particularly noteworthy in the context of reaction rate calculations for polyatomic systems. The equations of motion of the MCTDH approach show matrix elements of the potential energy

8

$V(x_1, .., x_f)$ as, for example,

$$\left\langle \prod_{\kappa=1}^{f} \phi_{j_\kappa}^{(\kappa)} \middle| V(x_1, .., x_f) \middle| \prod_{\kappa=1}^{f} \phi_{m_\kappa}^{(\kappa)} \right\rangle . \tag{5}$$

For reactive systems the potential energy functions $V(x_1, .., x_f)$ are typically involved functions of all coordinates and the correlation DVR (CDVR) [96] provided an efficient quadrature used in the MCTDH reaction rate calculations to evaluate these potential energy matrix elements. CDVR employs a layered time-dependent grid representation corresponding the MCTDH wavefunction: small sets of n_κ grid points $\xi_j^{(\kappa)}$ corresponding to the n_κ SPF $\phi_j^{(\kappa)}$ and large sets of N_κ grid points $\Xi_l^{(\kappa)}$ corresponding to the N_κ primitive time-independent basis functions $\chi_l(x_\kappa)$ are used simultaneously. The combined use of the f grids $(\Xi_{l_1}^{(1)}, \xi_{j_2}^{(2)}, \xi_{j_3}^{(3)} .., \xi_{j_f}^{(f)})$, $(\xi_{j_1}^{(1)}, \Xi_{l_2}^{(2)}, \xi_{j_3}^{(3)}, .., \xi_{j_f}^{(f)})$, .. , $(\xi_{j_1}^{(1)}, \xi_{j_2}^{(2)}, \xi_{j_3}^{(3)}, .., \Xi_{j_f}^{(f)})$ and the grid $(\xi_{j_1}^{(1)}, \xi_{j_2}^{(2)}, .., \xi_{j_f}^{(f)})$ yields a efficient and accurate quadrature [94–98].

A second numerical technique, the rigorous statistical sampling approach [54, 55, 99], contributes to the efficiency of reaction rate calculations which explicitly considered all $J \neq 0$ total angular momentum states [54, 55, 65, 67] or higher levels of vibrational excitation present at high temperatures [70]. It basically is a scheme for the efficient evaluation of the trace. Consider a complete basis set $\{|\chi_l\rangle\}$ of size N and an operator $\hat{A}$ represented in this basis,

$$A_{mn} = \left\langle \chi_m \middle| \hat{A} \middle| \chi_n \right\rangle . \tag{6}$$

Introducing M statistical functions

$$|\phi_j> = \sum_l (-1)^{\alpha_l(j)} \cdot |\chi_l> , \quad j = 1, 2, .., M , \tag{7}$$

where $\alpha_l(j)$ denotes an integer random number, one finds that the average of their expectation values

$$\langle A \rangle_j = \left\langle \phi_j \middle| \hat{A} \middle| \phi_j \right\rangle = \sum_{n,m} (-1)^{\alpha_m(j)+\alpha_n(j)} A_{mn} \tag{8}$$

converges in the limit of large M towards the trace of $\hat{A}$

$$\lim_{M \to \infty} \frac{1}{M} \sum_{j=1}^{M} \langle A \rangle_j =$$

$$\sum_{n,m} A_{mn} \left(\lim_{M \to \infty} \frac{1}{M} \sum_{j=1}^{M} (-1)^{\alpha_m(j)+\alpha_n(j)} \right) =$$

$$\sum_{n,m} A_{mn} \delta_{nm} = tr\left(\hat{A} \right) . \tag{9}$$

The efficiency of the sampling scheme depends on the choice of the basis functions χ_l. If A_{mn} is diagonal, all $\langle A \rangle_j$ are equal and only a single sample, i.e. $M = 1$, is required. More generally, the variance of trace computed using M sample depends

only on the off-diagonal elements of A_{mn} [54]. Thus, the sampling scheme is ideal for the description of weakly correlated degrees of freedom where approximate eigenfunctions of the operator in question, e.g. the Wigner rotation matrices for the description of rotational motion if the Hamiltonian is considered, are known. The scheme can favorably be combined with the MCTDH approach for the evaluation of flux correlations functions [54, 55] and the calculation of partition functions [99].

2.4.   *Quantum effects in reaction rates: Conclusions*

As already discussed in Sect.2.2, a large number of detailed theoretical studies of thermal rate constants was presented for diverse reactions within the last two decade. Based on these results, a consistent picture emerged which allows on to understand in detail diverse quantum effects on reaction rates as well as the relevance of the coupling of internal and rotational motion. These results are of particular interest considering the a larger community of theoretically interested chemists: understanding when computationally less demanding approaches and simplified models, standard classical harmonic transition theory in particular, can safely be employed is of crucial importance for the investigation larger molecular systems of applied chemical or biochemical interest. The present section therefore tries to concisely summarize central conclusions obtained from rigorous reaction rate calculations.

Quantum mechanical tunneling typically results in a significant increase of thermal rate constants of hydrogen transfer processes at temperatures below 500 K. Comparing the results of accurate reaction rate calculations with results obtained by harmonic TST which do not account for quantum tunneling, quantum effects typically increase of k(T) by factors of about 5 to 10 at room temperature. The results for the $H + CH_4$ reaction displayed in Fig.1 provide a typical example. Similar results were found for a number of other hydrogen-transferring reactions, e.g., $HCl + OH \rightarrow Cl + H_2O$ [67] or $O + CH_4 \rightarrow OH + CH_3$ [71]. While tunneling significantly enhances the reaction rates at temperatures below about 400 K, it tends to become less important above about 500 K and typically stops to be significant somewhere between 500 K and 1000 K. It should be noted that all these reactions show a rather imaginary normal mode frequency ω_{imag} at the transition state which significantly exceeds the available thermal energy $k_B T$: ω_{imag} equals 1414 cm^{-1} for $H + CH_4 \rightarrow H_2 + CH_3$ [19], 1549 cm^{-1} for $O + CH_4 \rightarrow OH + CH_3$ [73], 1192 cm^{-1} for $H_2 + OH \rightarrow H + H_2O$ [100], or 1441 cm^{-1} for $H_2 + Cl \rightarrow H + HCl$ [101].

While quantum mechanical tunneling clearly is a prominent effect in reactions where hydrogen atoms are transferred, it is not particularly important for reactions where exclusively heavy atoms are involved. Despite opposite claims for processes as the dissociative adsorption of N_2 on a Ru-surface, quantum effects on the rate constants of such reactive processes are comparatively small [82]. As an example, Fig.2 displays the thermal rate constant for the dissociative adsorption of N_2 on a stepped Ru-surface [82]. Here the enhancement due to quantum tunneling does not exceed 40 percent even at temperatures as low as 200 K. A simple Wigner tunneling correction [102]

$$\frac{k_{QM}}{k_{TST}} = 1 + \frac{1}{24}\left(\frac{\omega_{imag}}{k_B T}\right)^2 \tag{10}$$

is already sufficient to describe the quantum effects quite well, since here the imaginary frequency, $\omega_{imag} = 409$ cm^{-1} is much smaller compared to ω_{imag} for hydrogen transfer reactions. Thus, the imaginary normal mode frequency at the transition
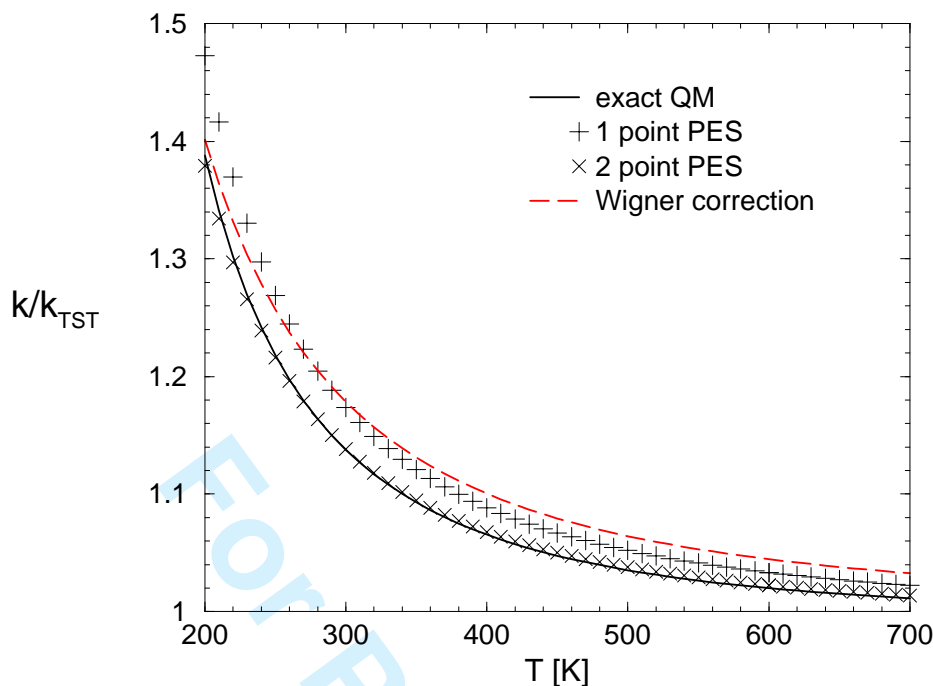
Figure 2. Thermal rate constants $k(T)$ for the dissociative adsorption of N_2 on a stepped Ru surface [82, 85]. The ratio $k(T)/k_{TST}$ relative the transition state theory rate constant k_{TST} is displayed. Results from exact quantum mechanical calculations (full line) and the Wigner correction (dashed line) for the fully interpolated PES are given as well as quantum mechanical results calculated for PESs employing only one or two reference points in the modified Shepard interpolation.

state provides a good indication for the size of the tunneling effects to be expected.

Studying a reaction where quantum effects are important, one might consider to avoid rigorous full-dimensional calculations and to employ a reduced-dimensional description to account for the quantum effects present. Several reduced-dimensional models were investigated for benchmark reactions as $H + CH_4 \rightarrow H_2 + CH_3$ [78, 103–109] or $H_2 + OH \rightarrow H + H_2O$ [110, 111] and compared to accurate full-dimensional results. Depending on the choice of the coordinates explicitly included and the modeling used to account for the neglected degrees of freedom, results of varying accuracy have been obtained. Approximate but full-dimensional transition state based theories tended to provide more reliable results for thermal rate constants [13–16, 112]. Using well-adjusted reduced-dimensional models or transition state based approximate theories accounting for quantum effects, approximate reaction rate calculations rather predictably achieve agreements with accurate results within a factor of about two to three and in fortuitous cases even significantly better agreements were found. However, due to the intrinsic limitations of both types of approximate approaches, systematic improvement of such approximate results towards the accurate ones is generally not possible.

The above discussion about quantum effects in reaction rates has focused on tunneling. Zero point energy effects are, in principle, as least as important. Considering the $H + CH_4 \rightarrow H_2 + CH_3$ as a typical example, the vibrationally adiabatic barrier height, which includes zero point energy in harmonic approximation, is 13.8 $kcal/mol$ while the corresponding pure potential energy barrier is 14.9 $kcal/mol$ [19]. Thus, zero point energy effects lower the effective barrier by $\Delta E_0 = -1.1$ $kcal/mol$ which corresponds to an increase of the room temperature rate of about a factor 7 ($= e^{-\Delta E_0/k_B T}$). However, since harmonic estimates for zero point energy effects are typically included even into the "classical" TST rate constants, this effect is usually not considered as a "quantum effect".

While zero point energy effects can be easily included on the level of the harmonic approximation if the vibrational frequencies of the reactants and at the transition state geometry are known, a rigorous treatment accounting for anharmonic effects requires a more elaborate description. Since reactive and vibrational motion in the barrier region are usually strongly coupled, descriptions beyond the most simple harmonic approximation require truly multi-dimensional quantum dynamics calculations. Here it was found that the anharmonicities in principle have a sizeable effect on the zero point energies (e.g., around 0.5 $kcal/mol$ for CH_4 [69, 99] and the $H + CH_4$ transition state [70] at the Jordan-Gilbert PES [72]), but these effects cancel out quite well when the differences between the transition state energies and the reactant energies are considered [69, 70]. Thus, approximate calculations can typically disregard such anharmonic effects as long as it is consistently done in the reactant partition function and the $N(E)$ computation.

The effect of anharmonicities on the vibrational excitation energies present in the different vibrational contributions to $N(E)$ [70, 74] and the reactant partition function [99] were found to be irrelevant at the typical temperatures considered in quantum reaction rate calculations. Moreover, the contributions of the different vibrational states of the activated complex to $k(T)$ and $N(E)$ were found to show approximately equal enhancement factors due to quantum tunneling [70, 74]. Thus, calculating thermal rate constants as

$$k(T) = \frac{Q^{\ddagger}_{rovib}}{Q_r} \frac{1}{2\pi} \int dE \ N_{GS}(E) \ e^{-\frac{E}{k_B T}} \ , \tag{11}$$

where $Q^{\ddagger}_{rovib}$ is the rovibrational partition function at the transition state, Q_r is the partition function of the reactants, and $N_{GS}(E)$ is the $N(E)$ contribution of the ground vibrational state of the activated complex (i.e., the contribution of the pair of thermal flux eigenstates showing the largest absolute eigenvalues), typically provides an excellent approximation to the exact $k(T)$.

Isotope effects in hydrogen transfer reactions as $H/D + CH_4$ or $H_2/HD/D_2 + CH_3$ were straightforwardly analyzed based on the above ideas [74, 75]: primary isotope effects are strongly influenced by quantum mechanical tunneling since the mass of the transferring particle is varied. In contrast, secondary isotope effects are well described by standard harmonic TST: here only the zero point energies changes which is well described by the TST treatment as discussed above.

The above discussion focused on the internal degrees of freedom of the reacting system. A rigorous treatment has to consider overall rotation, i.e. rotation of the entire system of reacting molecules. In a TST description, overall rotation is generally considered to be separable from internal motion and a rigid rotor model is employed for the description of the rotational motion. Then the thermal rate constant can be calculated as

$$k_{TST}(T) = \frac{Q^{\ddagger}_{rot} Q^{\ddagger}_{vib}}{2\pi Q_r} \ k_B T \ \exp(-E_b/k_B T) \tag{12}$$

where E_b is the (vibrationally adiabatic) barrier height and $Q^{\ddagger}_{rot}$ and $Q^{\ddagger}_{vib}$ are the rotational and vibrational partition functions of the transition state, respectively.

The separability of overall rotation and internal motion is frequently also assumed in otherwise rigorous quantum reaction rate calculations. This approach is called

J-shifting [56]. Then k(T) is calculated as

$$k_{J-shifting}(T) = \frac{Q_{rot}^{\ddagger}Q_{vib}^{\ddagger}}{2\pi Q_r} \int dE \ N_{J=0}(E) \ e^{-\frac{E}{k_B T}} \tag{13}$$

where $N_{J=0}(E)$ is the cumulative reaction probability computed for vanishing total angular momentum J. Since the J-shifting approach significantly reduces the numerical effort compared to calculations considering all J values explicitly, this approximation is highly attractive and its validity has been investigated in great detail for reactions as $O + HCl \rightarrow OH + Cl$ [45, 47, 54, 55, 62, 113], $H_2 + Cl \rightarrow H + HCl$ [59–61], $H_2 + OH \rightarrow H + H_2O$ [64, 65], $HCl + OH \rightarrow Cl + H_2O$ [67].

The accuracy of the J-shifting scheme was found to be directly be related to ability to define unique moments of inertia for the activated complex. If the activated complex is rigid and the moments of inertia vary only weakly over the dynamical relevant region, the J-shifting approach yields accurate results. Considering that for a nonlinear transition state the rotational partition is (in the classical limit) given by

$$Q_{rot}^{\neq}(T) = \sqrt{\frac{\pi(kT)^3}{8I_A I_B I_C}} \ , \tag{14}$$

where I_A, I_B, and I_C are the three principle moments of inertia of the activated complex, one can directly relate the error margin of the J-shifting approach to the variation of the moments of inertia during the time scale relevant for the determination of the reaction rate. This time scale is typically only in the range of a few ten femtoseconds. The J-shifting approach works particularly well for larger reactive systems since there all moments of inertia tend to be large and vary comparatively little in course of reaction.

Even if in cases where the transition state is only semirigid, the errors introduced be the J-shifting approach remain moderate: errors of 20 and 30 percent have found in the unfavorable cases as $O + HCl$ [55] and $H_2 + OH$ [65]. In these cases, more accurate results can be obtained employing the centrifugal sudden (CS) approximation [114–116]. Investigating reactions with linear transition states, the coordinate describing reaction around the linear axis must obviously be included in the explicit dynamical treatment. A J-shifting analogous procedure can then be employed to account for the two remaining rotational degrees of freedom [60] or one can resort to a CS description.

3. Potential energy surfaces for reaction rate calculations

3.1. *Constructing multi-dimensional PESs*

Considering the availability of accurate multi-dimensional PESs, the last decade witnessed tremendous progress. Until about ten years ago, accurate ab initio PESs were available only for selected three atom reactions. Meanwhile efficient techniques which allow one to construct truly multi-dimensional PESs based on a comparatively moderate amount of electronic structure calculations were developed.

The modified Shepard interpolation approach of Collins and coworkers [117–124] pioneered this development. In this approach, the potential energy surface (PES)

is constructed as the weighted sum of local contributions:

$$V(\mathbf{q}) = \sum_{i=1}^{N_{ref}} w_i(\mathbf{q}) \; V_{local}(\mathbf{q}, \mathbf{q}_i). \qquad (15)$$

Here the local potentials $V_{local}(\mathbf{q}, \mathbf{q}_i)$ provide accurate descriptions of the potential in the vicinity of the reference points $\mathbf{q}_i$ and the $w_i(\mathbf{q})$ are weighting functions guaranteeing a smooth interpolation of these local potentials. The local potentials are given as second order Taylor expansions and the required energies, gradients, and second derivatives (Hessians) at the reference points can be directly obtained from electronic structure calculations. Appropriate linear combinations of all inverse pairwise distances $1/r_{ij}$ provide optimal coordinates to be used in the harmonic expansion. This use of specific curvilinear coordinates allows one to include a significant part of anharmonicities already on the level of the contributions V_{local} of a single reference point. The quality of the interpolated PES depends on the position and number of reference points. By successively adding points, the quality of the PES can be improved until convergence (towards the limit given by the electronic structure theory employed). Combing the addition of new reference points with dynamical calculations which monitor the convergence and suggest the position of new reference points, a "semi-direct" approach interfacing electronic structure and dynamics calculations results.

Employing the Shepard interpolation approach, accurate PESs for the calculations of thermal rate constants of the four atom reaction $H_2 + OH \rightarrow H + H_2O$ [125–127] and the six atom reaction $H + CH_4 \rightarrow H_2 + CH_3$ [18, 19, 74, 75] were presented for the first time in 2000 and 2004, respectively.

More recently, another efficient scheme for the construction of multi-dimensional PES was developed by Bowman, Braams, and coworkers [128, 129]. It also employs dynamical calculations to suggest relevant geometries where electronic structure calculations are required, but then employs a fit to this data instead of an interpolation to construct the PES. The analytic form of the PES used in the fit is a polynomial depending on all the rescaled pairwise distances $e^{-\alpha \cdot r_{ij}}$ which form an over-complete set of coordinates. In the polynomials complete permutational symmetry of all identical atoms is enforced which drastically reduces the number of independent coefficients and thus allows one to use comparatively high order polynomials without requiring a prohibitively large amount of ab initio data.

The scheme was used to construct global PESs, e.g., for the $H + CH_4 \rightarrow H_2 + CH_3$ [130, 131] and $F + CH_4 \rightarrow HF + CH_3$ [132] reactions. While this fitting based approach is very successful for the construction of global PESs requiring in scattering calculations, the Shepard interpolation approach has a distinct advantage when considering reaction rate calculations: interpolation avoids errors in the barrier height and the transition state vibrational frequencies. Thus, the most crucial quantity in a k(T) calculation, the vibrationally adiabatic barrier height, is accurately reproduced by the interpolation approach while the fitting approach here introduces additional errors.

3.2.   *PESs designed for reaction rate calculations*

The thermal rate constant is determined by the dynamics in the vicinity of the reaction barrier. Thus, only the PES in this region really affects k(T). This fact simplifies the task of constructing an accurate PES to be used in reaction rate calculations. However, since the ratio of energy differences ΔE and the thermal

energy $k_B T$ enters into the rate constant roughly exponentially as $e^{-\frac{\Delta E}{k_B T}}$, very precise energy values are required. To accommodate these needs, a specific Shepard-interpolation based scheme for the construction of PESs specifically designed for reaction rate calculations was developed [133]. Application to the $H + CH_4 \rightarrow H_2 + CH_3$ reaction [19] and the dissociative adsorption of N_2 on a stepped Ru surface found that only a very small number of reference points must be employed in the Shepard interpolation to achieve accurate results.

This finding is directly related to the physical nature of the process and should be discussed in the following in more detail. Fig.1 shows the thermal rate constant computed for the $H + CH_4 \rightarrow H_2 + CH_3$ reaction on a fully converged Shepard-interpolated PES (solid line) and an approximate PES which is only based on 23 reference points located at the minimum energy path (MEP) (dashed line). One finds that already the approximate MEP based PES yields quite accurate k(T) results. Consequently, only a small number of additional reference points is required to perfectly converge the relevant PES completely and less than 50 symmetry unique reference points were used in the fully converged k(T) calculation. An even more extreme result can be seen if a reaction showing smaller quantum effects is studied. Fig.2 displays the thermal rate constant of the dissociative adsorption of N_2 on a stepped Ru surface. Here the full line shows results calculated on the converged PES while the symbols display results obtained for PESs based only on one or two reference points located close to the transition state. It is impressive to see that a single reference points is almost sufficient and that two reference points yield converged results. Considering the very nature of the transition state concept, these findings can be easily rationalized. Harmonic TST only requires the knowledge of the barrier height and the vibrational frequencies at the transition state: thus a PES based on a single reference point would be sufficient to compute k(T) within TST. The number of reference points required in the PES interpolation is therefore directly related to the extend of non-TST effects present in k(T).

4.   Conclusions and perspectives

The present article reviewed the development in accurate reaction rate calculations over the last one to two decades. Concluding the review, two aspects should be pointed out in particular:

- Studying a variety of gas phase reactions which involve three to six atoms, a consistent picture explaining the extend and importance of quantum effects seen in thermal rate constants has emerged. Effects resulting from zero point energy, tunneling, occupation of vibrationally excited states of the activated complex, or the coupling of internal motion and overall rotation have been studied and understood in detail.

- Reaction rate calculations based on the quantum transition state concept, modern quantum dynamics approaches (MCTDH) and PES construction techniques as well as high level ab initio calculation allow one to accurately predict thermal rate constants for gas phase reactions involving - presently - up to six atoms. Considering recent developments in quantum dynamics as the multi-layer MCTDH approach [93–95] and the ability of the Shepard-interpolation based schemes to efficiently construct high-dimensional PESs specifically designed for the use in reaction rate calculations, accurate calculations for system consisting of even more atoms are in reach.

Moreover, just recently MCTDH calculations propagating wave packets from the transition state to the asymptotic region obtained initial state-selected reac-

tion probabilities for the $H + CH_4 \rightarrow H_2 + CH_3$ [6, 7]. Based on older ideas [43, 134, 135], these calculations utilized the quantum transition concept to calculate state-specific quantities observed in scattering experiments and provided a perspective towards an accurate and fully state-resolved description of polyatomic reactions as $H + CH_4$, $Cl + CH_4$, or $F + CH_4$. Thus future studies might be able to combine transition state based ideas with state-selective scattering views to obtain an improved understanding of quantum state-specific chemistry.

5. Acknowledgments

References

[1] G. C. Schatz and A. Kuppermann, J. Chem. Phys. **65**, 4668 (1976).
[2] U. Manthe, T. Seideman, and W. H. Miller, J. Chem. Phys. **99**, 10078 (1993).
[3] D. Neuhauser, J. Chem. Phys. **100**, 9272 (1994).
[4] D. H. Zhang and J. Z. H. Zhang, J. Chem. Phys. **101**, 1146 (1994).
[5] F. Huarte-Larranaga and U. Manthe, J. Chem. Phys. **113**, 5115 (2000).
[6] G. Schiffel and U. Manthe, J. Chem. Phys. **132**, 191101 (2010).
[7] G. Schiffel and U. Manthe, J. Chem. Phys. **133**, 174124 (2010).
[8] H.-D. Meyer, U. Manthe, and L. S. Cederbaum, Chem. Phys. Lett. **165**, 73 (1990).
[9] U. Manthe, H.-D. Meyer, and L. S. Cederbaum, J. Chem. Phys. **97**, 3199 (1992).
[10] W. H. Miller, J. Chem. Phys. **61**, 1823 (1974).
[11] W. H. Miller, S. D. Schwartz, and J. W. Tromp, J. Chem. Phys. **79**, 4889 (1983).
[12] U. Manthe and W. H. Miller, J. Chem. Phys. **99**, 3411 (1993).
[13] J. Pu, J. Corchado, and D. Truhlar, J. Chem. Phys. **115**, 6266 (2001).
[14] J. Pu and D. Truhlar, J. Chem. Phys. **117**, 1479 (2002).
[15] S. Andersson *et al.*, J. Phys. Chem. A **113**, 4468 (2009).
[16] Y. V. Suleimanov, R. Collepardo-Guevara, and D. E. Manolopoulos, submitted to J. Chem. Phys. , (2010).
[17] E. J. Rackham, F. Huarte-Larranaga, and D. E. Manolopoulos, Chem. Phys. Lett. **343**, 356 (2001).
[18] T. Wu, H.-J. Werner, and U. Manthe, Science **306**, 2227 (2004).
[19] T. Wu, H.-J. Werner, and U. Manthe, J. Chem. Phys. **124**, 164307 (2006).
[20] T. Yamamoto, J. Chem. Phys. **33**, 281 (1960).
[21] W. H. Miller, Adv. Chem. Phys. **101**, 853 (1997).
[22] W. H. Miller, J. Phys. Chem. A **102**, 793 (1998).
[23] W. H. Miller, J. Chem. Soc. Faraday Trans. **93**, 685 (1998).
[24] U. Manthe, J. Theo. Comp. Chem. **1**, 153 (2002).
[25] F. Huarte-Larranaga and U. Manthe, Z. Phys. Chem. **221**, 171 (2007).
[26] T. J. Park and J. C. Light, J. Chem. Phys. **88**, 4897 (1988).
[27] R. E. Wyatt, Chem. Phys. Lett. **121**, 302 (1985).
[28] T. J. Park and J. C. Light, J. Chem. Phys. **85**, 5870 (1986).
[29] G. Wahnström and H. Metiu, Chem. Phys. Lett. **134**, 531 (1987).
[30] T. J. Park and J. C. Light, J. Chem. Phys. **91**, 974 (1989).
[31] P. N. Day and D. G. Truhlar, J. Chem. Phys. **94**, 2045 (1991).
[32] T. J. Park and J. C. Light, J. Chem. Phys. **94**, 2946 (1991).
[33] T. J. Park and J. C. Light, J. Chem. Phys. **96**, 8853 (1992).
[34] P. N. Day and D. G. Truhlar, J. Chem. Phys. **95**, 5097 (1991).
[35] N. Rom, N. Moiseyev, and R. Lefebvre, J. Chem. Phys. **96**, 8307 (1992).
[36] M. Thachuk and G. C. Schatz, J. Chem. Phys. **97**, 7297 (1992).
[37] T. Seideman and W. H. Miller, J. Chem. Phys. **96**, 4412 (1992).
[38] T. Seideman and W. H. Miller, J. Chem. Phys. **97**, 2499 (1992).
[39] U. Manthe, T. Seideman, and W. H. Miller, J. Chem. Phys. **101**, 4759 (1994).
[40] U. Manthe, J. Chem. Phys. **102**, 9205 (1995).
[41] W. H. Thompson and W. H. Miller, J. Chem. Phys. **102**, 7409 (1995).
[42] U. Manthe and F. Matzkies, Chem. Phys. Lett. **252**, 71 (1996).
[43] D. H. Zhang and J. C. Light, J. Chem. Phys. **104**, 6184 (1996).
[44] F. Matzkies and U. Manthe, J. Chem. Phys. **106**, 2646 (1997).
[45] W. H. Thompson and W. H. Miller, J. Chem. Phys. **106**, 142 (1997).

[46] S. M. Miller and T. Carrington, Chem. Phys. Lett. **267**, 417 (1997).
[47] B. Poirier, J. Chem. Phys. **108**, 5216 (1998).
[48] F. Matzkies and U. Manthe, J. Chem. Phys. **108**, 4828 (1998).
[49] U. Manthe and F. Matzkies, Chem. Phys. Lett. **282**, 442 (1998).
[50] K. M. Forsythe and S. K. Gray, J. Chem. Phys. **112**, 2623 (2000).
[51] M. Caspary, L. Berman, and U. Peskin, Isr. J. Chem. **42**, 237 (2003).
[52] D. M. Medvedev and S. K. Gray, J. Chem. Phys. **120**, 9060 (2004).
[53] U. Manthe, J. Chem. Phys. **128**, 064108 (2008).
[54] F. Matzkies and U. Manthe, J. Chem. Phys. **110**, 88 (1999).
[55] F. Matzkies and U. Manthe, J. Chem. Phys. **112**, 130 (2000).
[56] J. M. Bowman, J. Phys. Chem. **95**, 4960 (1991).
[57] G. C. Schatz and H. Elgersma, Chem. Phys. Lett. **21**, 73 (1980).
[58] S. P. Walch and T. H. Dunning, J. Chem. Phys. **72**, 1303 (1980).
[59] H. Wang, W. H. Thompson, and W. H. Miller, J. Chem. Phys. **107**, 7194 (1997).
[60] U. Manthe, W. Bian, and W. Werner, Chem. Phys. Lett. **313**, 647 (1999).
[61] U. Manthe, G. Cappecchi, and H.-J. Werner, Phys. Chem. Chem. Phys. **5026**, 2004 (2004).
[62] W. H. Thompson and W. H. Miller, J. Chem. Phys. **107**, 2164 (1997).
[63] D. H. Zhang and J. C. Light, J. Chem. Phys. **106**, 551 (1997).
[64] D. H. Zhang, J. C. Light, and S.-Y. Lee, J. Chem. Phys. **109**, 79 (1998).
[65] U. Manthe and F. Matzkies, J. Chem. Phys. **113**, 5725 (2000).
[66] J. C. Light and D. H. Zhang, Faraday Discussions **110**, 105 (1998).
[67] F. Huarte-Larranaga and U. Manthe, J. Chem. Phys. **118**, 8261 (2003).
[68] F. Huarte-Larranaga and U. Manthe, J. Phys. Chem. A **105**, 2522 (2001).
[69] J. M. Bowman *et al.*, J. Chem. Phys. **114**, 9683 (2001).
[70] F. Huarte-Larranaga and U. Manthe, J. Chem. Phys. **116**, 2863 (2002).
[71] F. Huarte-Larranaga and U. Manthe, J. Chem. Phys. **117**, 4635 (2002).
[72] M. Jordan and R. Gilbert, J. Chem. Phys. **102**, 5669 (1995).
[73] J. Espinosa-Garcia and J. C. Garcia-Bernaldez, Phys. Chem. Chem. Phys. **2**, 2345 (2000).
[74] R. van Harrevelt, G. Nyman, and U. Manthe, J. Chem. Phys. **126**, 084303 (2007).
[75] G. Nyman, R. van Harrevelt, and U. Manthe, J. Phys. Chem. A **111**, 10331 (2007).
[76] M. Moix and F. Huarte-Larranaga, Chem. Phys. **351**, 65 (2008).
[77] N. Faginas, F. Huarte-Larranaga, and A. Lagana, Chem. Phys. Lett. **464**, 249 (2008).
[78] L. Zhang, Y. Lu, D. H. Zhang, and S.-Y. Lee, J. Chem. Phys. **127**, 234313 (2007).
[79] G. Schiffel, U. Manthe, and G. Nyman, J. Phys. Chem. A **114**, 9617 (2010).
[80] G. Schiffel and U. Manthe, J. Chem. Phys. **132**, 084103 (2010).
[81] D. H. Zhang, J. C. Light, and S.-Y. Lee, J. Chem. Phys. **111**, 5741 (1999).
[82] R. van Harrevelt, K. Honkala, J. K. Nørskov, and U. Manthe, J. Chem. Phys. **122**, 234702 (2005).
[83] H. Wang, D. E. Skinner, and M. Thoss, J. Chem. Phys. **125**, 174502 (2006).
[84] I. R. Craig, M. Thoss, and H. Wang, J. Chem. Phys. **127**, 144503 (2007).
[85] R. van Harrevelt, K. Honkala, J. K. Nørskov, and U. Manthe, J. Chem. Phys. **124**, 026102 (2006).
[86] M. Topaler and N. Makri, J. Chem. Phys. **101**, 7500 (1994).
[87] D. O. Harris, G. G. Engerholm, and W. D. Gwinn, J. Chem. Phys. **43**, 1515 (1965).
[88] A. S. Dickinson and P. R. Certain, J. Chem. Phys. **49**, 4209 (1968).
[89] J. C. Light, I. P. Hamilton, and J. V. Lill, J. Chem. Phys. **82**, 1400 (1985).
[90] D. Kosloff and R. Kosloff, J. Comp. Phys. **52**, 35 (1983).
[91] M. Ehara, H.-D. Meyer, and L. S. Cederbaum, J. Chem. Phys. **105**, 8865 (1996).
[92] M. H. Beck, A. Jäckle, G. A. Worth, and H.-D. Meyer, Physics Reports **324**, 1 (2000).
[93] H. Wang and M. Thoss, J. Chem. Phys. **119**, 1289 (2003).
[94] U. Manthe, J. Chem. Phys. **128**, 164116 (2008).
[95] U. Manthe, J. Chem. Phys. **130**, 054109 (2009).
[96] U. Manthe, J. Chem. Phys. **105**, 6989 (1996).
[97] R. van Harrevelt und U. Manthe, J. Chem. Phys. **121**, 5623 (2004).
[98] R. van Harrevelt and U. Manthe, J. Chem. Phys. **123**, 064106 (2005).
[99] U. Manthe and F. Huarte-Larranaga, Chem. Phys. Lett. **349**, 321 (2001).
[100] M. Yang, D. H. Zhang, M. A. Collins, and S.-Y. Lee, J. Chem. Phys. **115**, 174 (2001).
[101] W. Bian and H.-J. Werner, J. Chem. Phys. **112**, 220 (2000).
[102] E. Wigner, Z. Phys. Chem. B. **19**, 203 (1932).
[103] T. Takayanagi, J. Chem. Phys. **104**, 2237 (1996).
[104] H.-G. Yu and G. Nyman, J. Chem. Phys. **111**, 3508 (1999).
[105] M. Wang, Y. Li, J. Zhang, and D. Zhang, J. Chem. Phys. **113**, 1802 (2000).
[106] D. Wang and J. M. Bowman, J. Chem. Phys. **115**, 2055 (2001).
[107] J. Palma, J. Echave, and D. C. Clary, J. Phys. Chem. A **106**, 8256 (2002).
[108] M. Wang and J. Zhang, J. Chem. Phys. **117**, 3081 (2002).
[109] M. Yang, D. H. Zhang, and S.-Y. Lee, J. Chem. Phys. **117**, 9539 (2002).
[110] D. C. Clary, J. Chem. Phys. **95**, 7298 (1991).
[111] D. Wang and J. M. Bowman, J. Chem. Phys. **96**, 8906 (1992).
[112] Y. Zhao, T. Yamamoto, and W. H. Miller, J. Chem. Phys. **120**, 3100 (2004).
[113] K. Nobudsada and H. Nakamura, J. Chem. Phys. **103**, 6715 (1999).
[114] R. T. Pack, J. Chem. Phys. **60**, 633 (1974).
[115] P. McGuire and D. J. Kouri, J. Chem. Phys. **60**, 2488 (1974).
[116] M. C. Colton and G. C. Schatz, Int. J. Chem. Kinet. **18**, 961 (1986).
[117] J. Ischtwan and M. A. Collins, J. Chem. Phys. **100**, 8080 (1994).
[118] M. J. T. Jordan, K. C. Thompson, and M. A. Collins, J. Chem. Phys. **102**, 5647 (1995).
[119] M. J. T. Jordan, K. C. Thompson, and M. A. Collins, J. Chem. Phys. **103**, 9669 (1995).
[120] M. J. T. Jordan and M. A. Collins, J. Chem. Phys. **104**, 4600 (1996).

[121] K. C. Thompson and M. A. Collins, J. Chem. Soc. Faraday Trans. **93**, 871 (1997).
[122] K. C. Thompson, M. J. T. Jordan, and M. A. Collins, J. Chem. Phys. **108**, 564 (1998).
[123] K. C. Thompson, M. J. T. Jordan, and M. A. Collins, J. Chem. Phys. **108**, 8302 (1998).
[124] R. P. A. Bettens and M. A. Collins, J. Chem. Phys. **111**, 816 (1999).
[125] D. H. Zhang, M. A. Collins, and S.-Y. Lee, Science **290**, 961 (2000).
[126] M. Yang, D. H. Zhang, M. A. Collins, and S.-Y. Lee, J. Chem. Phys. **114**, 4759 (2001).
[127] D. H. Zhang, M. Yang, and S.-Y. Lee, J. Chem. Phys. **116**, 2388 (2002).
[128] A. Brown *et al.*, J. Chem. Phys. **121**, 4105 (2004).
[129] B. J. Braams and J. M. Bowman, Int. Rev. Phys. Chem. **28**, 577 (2009).
[130] X. Zhang, B. J. Braams, and J. M. Bowman, J. Chem. Phys. **124**, 021104 (2006).
[131] Z. Xie, J. M. Bowman, and X. Zhang, J. Chem. Phys. **125**, 133120 (2006).
[132] G. Czako, B. C. Shepler, B. J. Braams, and J. M. Bowman, J. Chem. Phys. **130**, 0884301 (2009).
[133] T. Wu and U. Manthe, J. Chem. Phys. **119**, 14 (2003).
[134] U. Manthe, Chem. Phys. Lett. **241**, 497 (1995).
[135] F. Huarte-Larranaga and U. Manthe, J. Chem. Phys. **123**, 204114 (2005).

1
2
3
4
5
6
7
8
9
10
11
12
13
14
15
16
17
18
19
20
21
22
23
24
25
26
27
28
29
30
31
32
33
34
35
36
37
38
39
40
41
42
43
44
45
46
47
48
49
50
51
52
53
54
55
56
57
58
59
60